J. Am. Soc. Mass Spectrom. (2012) 23:2063–2074
DOI: 10.1007/s13361-012-0492-x

RESEARCH ARTICLE

The Radical Ion Chemistry of *S*-Nitrosylated Peptides

Andrew W. Jones, Peter J. Winn, Helen J. Cooper

School of Biosciences, College of Life and Environmental Sciences, University of Birmingham, Edgbaston, Birmingham, B15 2TT, United Kingdom

Abstract

The radical ion chemistry of a suite of *S*-nitrosopeptides has been investigated. Doubly and triply-protonated ions of peptides NYCGLPGEYWLGNDK, NYCGLPGEYWLGNDR, NYCGLPGERWLGNDR, NACGAPGEKWAGNDK, NYCGLPGEKYLGNDK, NYGLPGCEKWYGNDK and NYGLPGEKWYGCNDK were subjected to electron capture dissociation (ECD), and collision-induced dissociation (CID). The peptide sequences were selected such that the effect of the site of *S*-nitrosylation, the nature and position of the basic amino acid residues, and the nature of the other amino acid side chains, could be interrogated. The ECD mass spectra were dominated by a peak corresponding to loss of $^{\bullet}$NO from the charge-reduced precursor, which can be explained by a modified Utah-Washington mechanism. Some backbone fragmentation in which the nitrosyl modification was preserved was also observed in the ECD of some peptides. Molecular dynamics simulations of peptide ion structure suggest that the ECD behavior was dependent on the surface accessibility of the protonated residue. CID of the *S*-nitrosylated peptides resulted in homolysis of the S–N bond to form a long-lived radical with loss of $^{\bullet}$NO. The radical peptide ions were isolated and subjected to ECD and CID. ECD of the radical peptide ions provided an interesting comparison to ECD of the unmodified peptides. The dominant process was electron capture without further dissociation (ECnoD). CID of the radical peptide ions resulted in cysteine, leucine, and asparagine side chain losses, and radical-induced backbone fragmentation at tryptophan, tyrosine, and asparagine residues, in addition to charge-directed backbone fragmentation.

Key words: *S*-nitrosylation, Cysteine, Proteomics, CID, ECD, FT-ICR, FT-MS, Fourier transform ion cyclotron resonance, Gas-phase reactions, Molecular dynamics, Radical ions

Introduction

S-nitrosylation is a ubiquitous post-translational modification (PTM), fundamental for function and modulation in a wide array of proteins [1]. *S*-nitrosylation is formed by the reaction of nitric oxide (NO)—a signaling molecule that plays a diverse role in physiological processes e.g., immunological response, neurotransmission, and vascular homeostasis—with thiol functional groups on cysteine amino acid residues. The S–NO bond is highly labile. The average bond dissociation energy is 20–28 kcalmol^{-1} [2] (cf. RS-SR 70–74 kcalmol^{-1} [3]). Homolytic cleavage of the bond is observed following UV irradiation in solution [4] and collision-induced dissociation (CID) in the gas phase [5]. The characterization of *S*-nitrosylation is technically challenging, and methods have been reviewed by Torta et al. [6]. Li and co-workers described an electrospray Q-TOF strategy for direct analysis of *S*-nitrosylation, which relied on specific buffer conditions and mass spectrometry parameters [7]. Alternatively, the S–NO can be converted to an S-detectable tag e.g., the biotin switch method [8], the SNOSID (SNO Site IDentification) method [9], or the

Electronic supplementary material The online version of this article (doi:10.1007/s13361-012-0492-x) contains supplementary material, which is available to authorized users.

Correspondence to: Helen Cooper; *e-mail:* H.J.Cooper@bham.ac.uk

Received: 15 May 2012
Revised: 11 July 2012
Accepted: 20 July 2012
Published online: 4 October 2012

SHIPS (Site-specific High-throughput Identification of Protein *S*-nitrosylation) method [10].

Electron capture dissociation (ECD) [11, 12] mass spectrometry, and its sister technique electron transfer dissociation (ETD) [13], have emerged as useful methods for the analysis of protein PTMs, including phosphorylation [14, 15], and glycosylation [16, 17]. Nevertheless, ECD is not universally appropriate for the characterization of PTMs (e.g., tyrosine nitration [18]). In peptide/protein ECD, low energy electrons are captured by multiply-charged cations with subsequent cleavage of disulfide S–S and peptide backbone N–C_α bonds i.e., cleavage is radically driven. ECD is believed to occur via the Utah-Washington (UW) mechanism [19, 20] in which initial electron capture to a high-*n* Rydberg state is followed by transfer to either a Coulombic-stabilized amide π* orbital, rendering the amide bond superbasic, or a S–S σ* orbital. The superbasic amide anion radical or disulfide anion radical leads to N–C_α or S–S bond cleavage before ultimately abstracting a proton from an accessible site resulting in *c* and $z^\bullet$, or SH and $S^\bullet$, fragments.

Few studies have extensively investigated the effect of *S*-nitrosylation on MS/MS. Hao and Gross [5] investigated the CID of two *S*-nitrosopeptides derived from hemoglobin, one a truncated version of the other. They showed that the dominant fragmentation pathway was the neutral loss of $^\bullet$NO, resulting in the formation of a radical peptide ion. Further fragmentation (MS^3) of the radical peptide ions resulted in radical-type fragment ions (i.e. *c*/*z*/*x* ions). ETD of a 30-amino acid *S*-nitrosopeptide also resulted in favorable loss of $^\bullet$NO [21].

Here, we investigate the radical ion chemistry of a suite of *S*-nitrosopeptides. Doubly- and triply-charged *S*-nitrosopeptide ions were subjected to electron capture dissociation. The fragmentation observed is discussed in terms of the UW mechanism. Molecular dynamics simulations, which allow the prediction of the peptide ion structures, suggest that the surface accessibility of the protonated residues in the folded peptide determine the fragmentation patterns, due to either an increase in Coulombic stabilization consistent with the UW mechanism, or an inability to interact with the S–N bond hence favoring N–Cα bond fragmentation.

The *S*-nitrosopeptides were also subjected to CID, and in agreement with previous findings [5, 22], the dominant fragmentation channel was loss of $^\bullet$NO. The long-lived radical peptide ion was subjected to ECD, providing an interesting comparison with ECD of the unmodified (hydrogen abundant) peptide. ECD of the radical peptide ions resulted in a greater relative abundance of the charged-reduced precursor (the ECnoD ions). Finally, the radical peptide ions were subjected to further CID resulting in side chain losses and both radical-induced and charge-directed fragmentation.

Methods

Preparation of Synthetic Peptides

The peptides NYCGLPGEYWLGNDK, NYCGLPGEYWL GNDR, NYCGLPGERWLGNDR, NACGAPGEKWAGNDK, NYCGLPGEKYLGNDK, NYGLPGCEKWYGNDK, and NYGLPGEKWYGCNDK were synthesized by Alta Bioscience (Birmingham, UK) and Bachem (Weil am Rhein, Germany) and used without further purification. *S*-nitrosylation procedure was adapted from [5, 7]: 0.3 mg of each peptide was dissolved in 900 μL of 1 mM EDTA (Fisher Scientific, Leicestershire, UK) and 0.1 mM neocuproine (Sigma-Aldrich, Dorset, UK), and reacted with 100 μL 1 mM GSNO (Sigma-Aldrich) for 30 min at 39 °C in the dark. The reaction was quenched by freezing at −80 °C and no further purification was completed. The peptides were diluted to 2 pmol/μL in 49:49 % methanol (Fisher Scientific): water (J. T. Baker, Deventer, The Netherlands), and 2 % formic acid (Fisher Scientific).

Mass Spectrometry

All mass spectrometry experiments were performed on a Thermo Fisher LTQ FT Ultra mass spectrometer (Bremen, Germany). Samples were injected by use of an Advion Biosciences Triversa electrospray source (Ithaca, NY, USA) at a flow rate of ~200 nL/min. All mass spectra were acquired in the ICR cell with a resolution of 100,000 at *m*/*z* 400.

CID

CID experiments were performed in the linear ion trap and the fragments transferred to the ICR cell for detection. Automatic gain control (AGC) target was 2×10^5 with maximum fill time 1 s, isolation width was *m*/*z* 5. CID experiments were performed with helium gas at normalized collision energy 35 %, except for triply-charged *S*-nitrosylated peptides where 12 % was used. MS^3 CID was completed under the same conditions except an isolation width of *m*/*z* 10 was used for triply-charged *S*-nitrosylated peptides. Each MS/MS CID scan comprises 4 co-added microscans and each MS^3 CID scan comprises 10 co-added microscans. CID mass spectra shown comprise 30 average scans.

ECD

Precursor ions were isolated in the linear ion trap and transferred to the ICR cell for ECD. AGC was 2×10^5 with maximum fill time 1 s and the isolation width was *m*/*z* 5. Electrons for ECD were produced by an indirectly heated barium-tungsten cylindrical dispenser cathode (5.1 mm diameter, 154 mm from the cell, 1 mm off axis) (Heat-Wave Labs, Watsonville, CA, USA). The current across the cathode was ~1.1 A. Ions were irradiated with electrons for 70 ms at 5 % energy (corresponding to a cathode potential of −2.3375 to −2.775 V). MS^3 ECD was performed following MS/MS CID (CID conditions as above). Each MS/MS ECD scan comprises four co-added microscans and each MS^3 ECD scan comprises 10 co-added microscans. ECD mass spectra shown comprise 30 average scans.

All data were analysed using Xcalibur 2.1.0 software (Thermo Fisher Scientific), and manually searched for *a*, *b*,

$c^{\bullet}/c$, y, z/z' fragment ions using ProteinProspector ver. 5.7.2 software (UCSF, San Francisco, CA, USA).

Molecular Dynamics

All simulations were performed using Amber 10 and the ff99SB-ILDN forcefield [23]. The *S*-nitrosylation amino acids were added manually using previously calculated parameters [24]. Peptides underwent 500 cycles of steepest descent followed by 500 of conjugant gradient minimization followed by heating in a stepwise manner from 0 K up to 325 K. Each heating step consisted of 10,000 steps of 0.5 fs each (nstlim=10000, dt=0.0005), using a Langevin thermostat (ntt=3, gamma_ln=1.0) with no interacting solvent (igb=0). The production simulation was at 325 K for a total of 500 ns (100 stages of 5 ns containing 2,500,000 steps of 2 fs each), again using a Langevin thermostat with no interacting solvent. Clustering of the peptide structures obtained in 100 ns windows was completed using kclust (a k-means algorithm implemented in the MMTSB tool set [25]), using a 3 Å radius. The most representative structure (i.e., that with the lowest RMSD from the average structure for the cluster) found within the top (i.e., most abundant) cluster was then identified. The most representative structures from each 100 ns window were compared with each other using the RMSD calculator extension in visual molecular dynamics (VMD) to ensure that the final structure at 500 ns was fully converged. The surface accessibility of atoms and residues was calculated using a spherical probe of radius 1.4 Å using naccess and atom-to-atom distances were calculated using VMD.

Results

Electron Capture Dissociation of S-Nitrosylated Peptides

Figure 1 and Supplemental Figure 1 show the mass spectra obtained following ECD of the *S*-nitrosylated doubly- and triply-charged peptide ions. With the exception of $NYC_{NO}GLPGERWLGNDR$ and $NYC_{NO}GLPGEKYLGNDK$ (Figure 1b and c), there is a striking lack of backbone fragmentation for the doubly-charged peptides compared with their unmodified counterparts (Supplemental Figure 2). In all cases, the most abundant peak corresponds to the neutral loss of $^{\bullet}NO$ i.e., $[M - {}^{\bullet}NO + 2H]^{+}$ from the charge-reduced ion. Dominant $^{\bullet}NO$ neutral loss is observed following CID of *S*-nitrosopeptides [5, 22, 26–28], which might suggest a thermal process is occurring; however, no loss of $^{\bullet}NO$ from the doubly-charged precursor was observed and $[M - {}^{\bullet}NO + 2H]^{+}$ ions were observed when the energy of the electrons was reduced (Supplemental Figure 3).

The loss of $^{\bullet}NO$ can be explained by a modified UW mechanism, see Scheme 1. In this mechanism, initial electron capture to a high-*n* Rydberg state of the protonated basic amino acid residue or protonated N-terminus occurs followed by electron transfer to the RS–NO σ* orbital. Cleavage of the S–NO bond is followed by proton abstraction from an accessible site. Theoretical studies have suggested that the electron is captured directly into the S–S σ* orbital in 1 %–10 % of cases [29], and that may also be true for the S–NO σ* orbital. Once the radical NO has been lost, the remaining species is even-electron and would not dissociate. Recent quantum calculations have shown the weakness of the S–N bond in *S*-nitrosothiols is due to delocalization from the oxygen lone pair into the S–N σ* orbital [30] (i.e., the S–N σ* orbital is stabilized). Transfer of the electron to the S–N σ* orbital would therefore be in competition with transfer to a Coulomb-stabilized amide π* orbital.

Electron capture by the two doubly-charged nitrosylated peptides containing a single basic residue (Supplemental Figure 1a and b) resulted in small ammonia losses. The ammonia loss appears to originate from the site of protonation (N-terminus) at which the electron was captured [31]. (Further evidence for the site of electron capture comes from the uniquely C-terminal backbone fragments observed for $NYC_{NO}GLPGEYWLGNDK$). That is, electron transfer to the S–N σ* orbital or an amide π* orbital has not occurred. The ECD mass spectra (Figure 1 and Supplemental Figure 1a-d) also reveal small peaks corresponding to combined losses of $^{\bullet}NO$ and NH_3 from the charge-reduced precursor. In those cases, the α radical (resulting from N-terminal NH_3 loss) or the ε radical (resulting from NH_3 loss from lysine) must interact, directly or indirectly, with the sulfur atom with subsequent $^{\bullet}NO$ loss, or the $^{\bullet}NO$ loss is thermally driven and is distinct from the radically driven ammonia loss, or the $^{\bullet}NO$ loss is radically driven and ammonia loss is thermally driven.

Four of the doubly-charged peptides showed some, albeit reduced, backbone cleavage following electron capture, with two peptides retaining the $^{\bullet}NO$ modification. For $[NYC_{NO}GLPGEYWLGNDK + 2H]^{2+}$ and $[NYGLPGEKWYGC_{NO}NDK + 2H]^{2+}$, backbone cleavage was minimal. ECD of $[NYC_{NO}GLPGERWLGNDR + 2H]^{2+}$ resulted in 43 % sequence coverage (c.f. 93 % for the unmodified peptide). Both $[NYGLPGEKWYGC_{NO}NDK + 2H]^{2+}$ and $[NYC_{NO}GLPGERWLGNDR + 2H]^{2+}$ produced some backbone fragments minus $^{\bullet}NO$. These fragments presumably are derived from radically driven backbone fragmentation with concomitant thermally driven loss of $^{\bullet}NO$. The abundance of these fragments suggests that this is a minor pathway. ECD of $[NYC_{NO}GLPGEKYLGNDK + 2H]^{2+}$ resulted in 71 % sequence coverage (c.f. 86 % for the unmodified peptide). None of the backbone fragments exhibited loss of $^{\bullet}NO$; however, $^{\bullet}NO$ loss from the charge-reduced precursor remained the dominant fragment. These results suggest a competition between electron capture/transfer into either the RS-NO σ* orbital or the $N–C_{\alpha}$ π* orbital. With the exception of $[NYGLPGEKWYGC_{NO}NDK + 2H]^{2+}$, the ECD spectra which contained backbone fragments also contained peaks corresponding to the loss of SNO from the charge-reduced species. The presence of these peaks is evidence for a

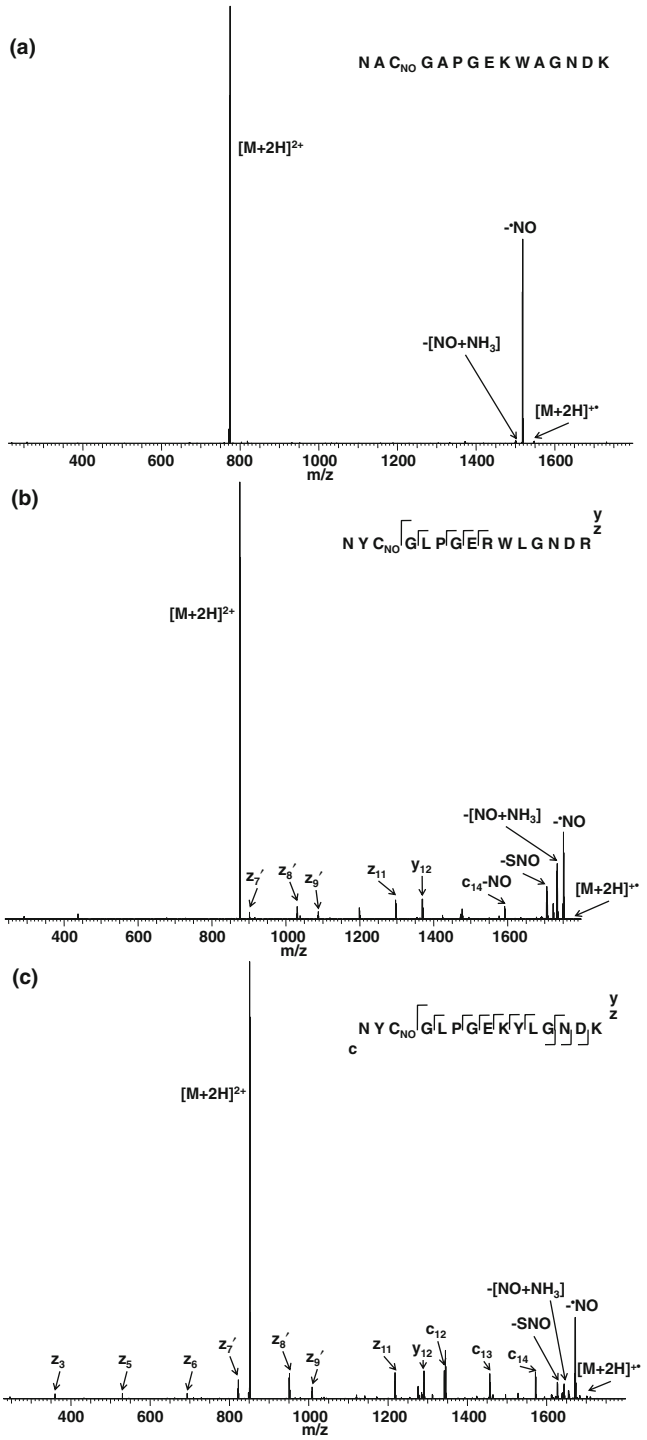

Figure 1. ECD mass spectra of *S*-nitrosylated peptide ions: **(a)** $[NAC_{NO}GAPGEKWAGNDK + 2H]^{2+}$; **(b)** $[NYC_{NO}GLP-GERWLGNDR + 2H]^{2+}$; **(c)** $[NYC_{NO}GLPGEKYLGNDK + 2H]^{2+}$. C_{NO} denotes *S*-nitrosylation

mobile radical. Scheme 2 shows the proposed pathway for loss of SNO: hydrogen abstraction results in the formation of a radical at the α position of the nitrosocysteine residue and cleavage of the C_β–S bond.

The ECD behavior of the nitrosylated peptides covers a spectrum, from dominant electron transfer to the S–N σ* orbital (in most cases) to a relatively even competition between transfer to the S–N σ* orbital and an amide π* orbital. In order to explain these behaviors, we considered the molecular structures of the peptides generated by molecular dynamics simulations, measuring the distance between groups of interest and their surface accessibility from the most representative structures. For $[NAC_{NO}GAPGEKWAGNDK + 2H]^{2+}$ (representative of the five peptides where no backbone fragmentation

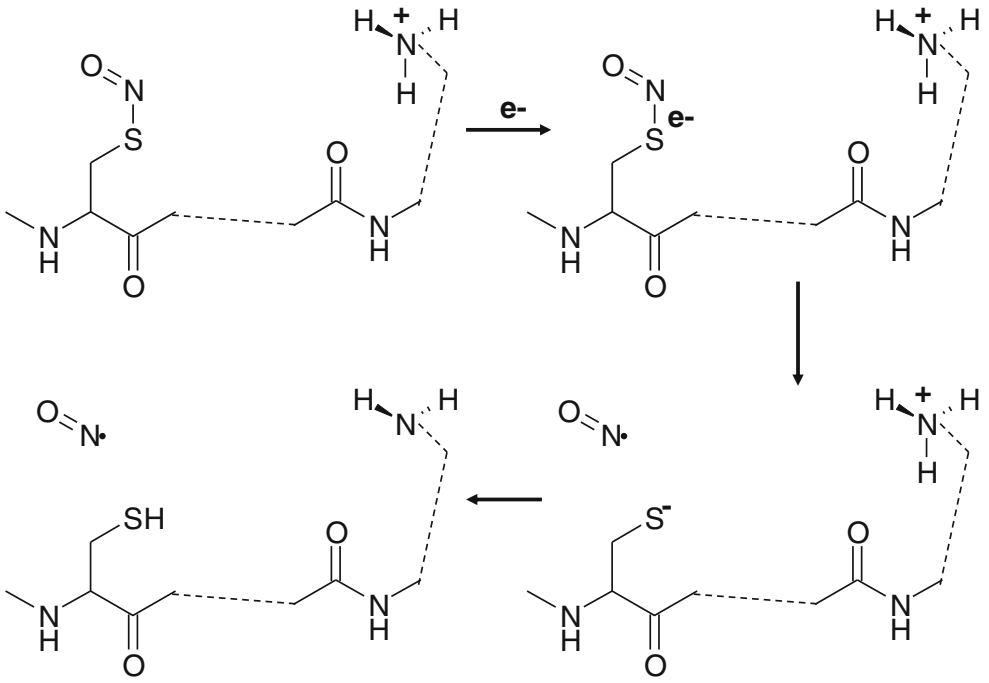

Scheme 1. Proposed mechanism of •NO loss following ECD of *S*-nitrosopeptides

was observed) (Figure 2a), the proton on the central lysine is close in space (4.3 Å) to the carbonyl of the nitrosocysteine and the C-terminal region of the peptide has a fairly open structure (surface accessibility of the polar atoms in the C-terminal lysine side chain was 68 $Å^2$). ECD of $[NYC_{NO}GLPGERWLGNDR + 2H]^{2+}$ ions resulted in backbone fragments in the region between Cys3 and Arg9. The predicted molecular structure of $[NYC_{NO}GLPGERWLGNDR + 2H]^{2+}$, Figure 2b, shows the protonated central arginine to be buried (surface accessibility of the polar atoms in the side chain was 21 $Å^2$) within the Cys3-Arg9 region of the peptide whereas the C-terminal region of the peptide is fairly open and the C-terminal arginine (surface accessibility of the polar atoms in the side chain was 45.64 $Å^2$) is not interacting closely with the peptide backbone. The predicted structure of $[NYC_{NO}GLPGEKYLGNDK + 2H]^{2+}$, Figure 2c, reveals the central protonated lysine to be buried (the surface accessibility of the polar atoms in the side chain was 0.00 $Å^2$) in the N-terminal region of the peptide and the C-terminal protonated lysine to be buried (the surface accessibility of the polar atoms in the side chain was 22 $Å^2$) in the C-terminal region of the peptide. For this species, backbone fragments were observed between Cys3 and Lys14. These data suggest that the observed backbone fragmentation is the result of limited accessibility of the protonation site. Either this limited accessibility inhibits electron transfer to the S–N σ* orbital or directs electron transfer to the amide π* orbital following electron capture at the protonation site, or these interactions increase the Coulomb stabilization of the amide π* orbital making electron transfer to that orbital more competitive. Molecular models for the remaining doubly-charged peptides were generated (Supplemental Figure 4a-d). The models support the above conclusions, with the exception of $[NYC_{NO}GLPGEYWLGNDK + 2H]^{2+}$. For that species, protonated Lys14 is buried (the surface accessibility of the polar atoms in the side chain was 18 $Å^2$) in the C-terminal region of the peptide however no fragments from that region were observed. However, as discussed above, the observed ammonia loss suggests that electron capture occurs at the N-

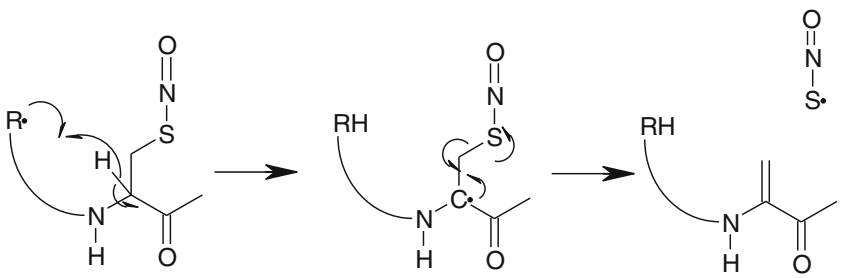

Scheme 2. Proposed mechanism of •SNO loss following ECD of *S*-nitrosopeptides

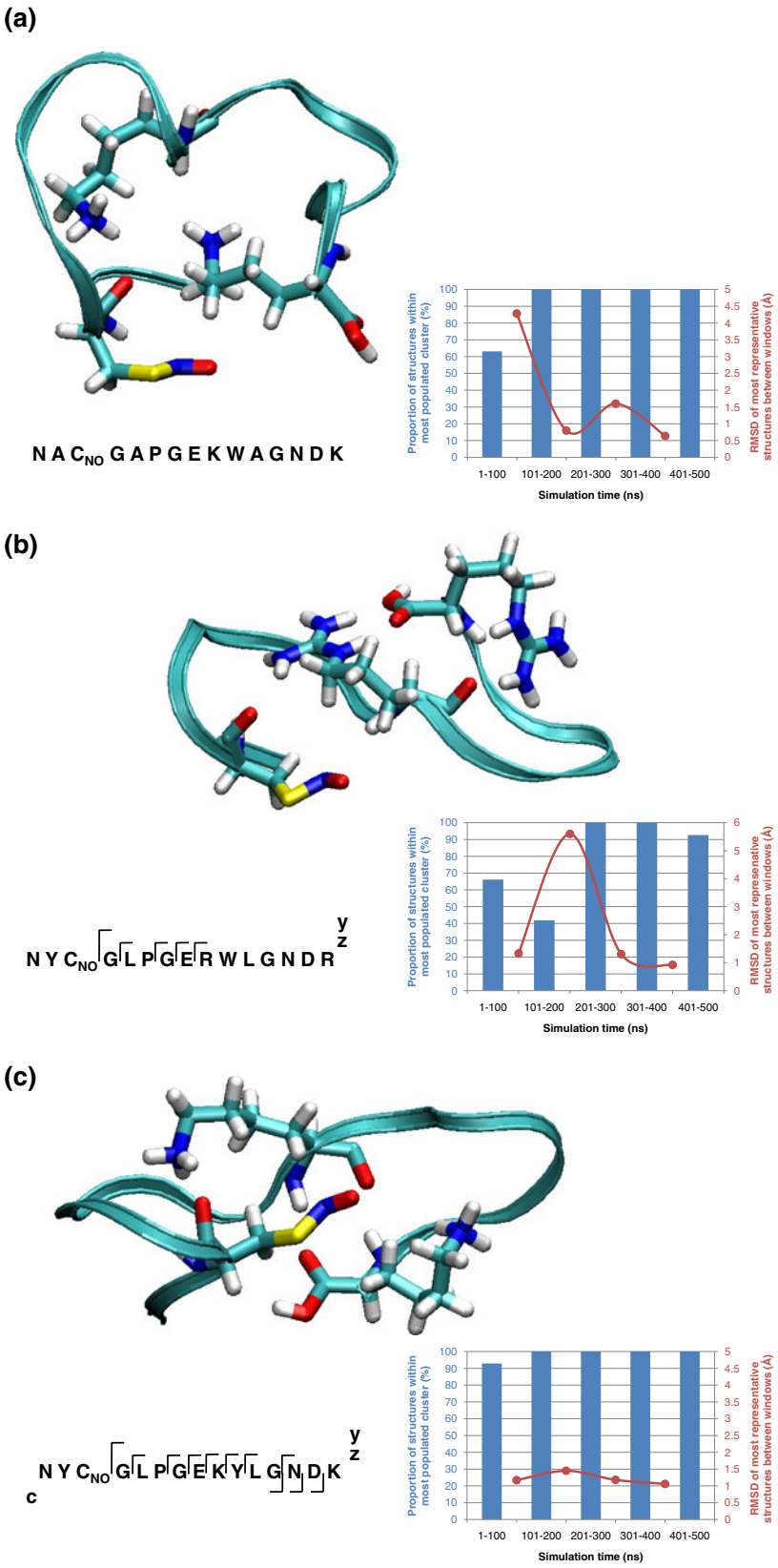

Figure 2. Molecular models of *S*-nitrosylated peptide ions: **(a)** $[NAC_{NO}GAPGEKWAGNDK + 2H]^{2+}$; **(b)** $[NYC_{NO}GLPGERWLGNDR + 2H]^{2+}$; **(c)** $[NYC_{NO}GLPGEKYLGNDK + 2H]^{2+}$. Graphs show the percentage of the most populated cluster within each timeframe along with RMSD of the representative structure of the window with respect to the representative structure of the previous window. Inset: summary of ECD fragmentation

terminus (the surface accessibility of the polar atoms within the N-terminal asparagine amino acid residue was 73 $Å^2$) rather than the protonated lysine.

ECD of the triply-charged *S*-nitrosylated peptide ions (Supplementary Figure 1e–i) are in stark contrast to their doubly-charged counterparts due to the much increased peptide sequence coverage observed (>50 % in all peptides). Three points should be noted: first, as with their doubly-charged counterparts, the most abundant fragment following ECD derives from the neutral loss of $^{\bullet}NO$ following electron capture, with the exception of $[NYC_{NO}GLPGEKYLGNDK + 3H]^{3+}$ where it is the second most abundant. Second, very few doubly-charged peptide backbone fragment ions are observed, and for the majority of the peptides, singly-charged backbone fragments have lost $^{\bullet}NO$. Third, as for the doubly-charged ions, $NYC_{NO}GLPGERWLGNDR$ and $NYC_{NO}GLPGEKYLGNDK$ behave differently from the other *S*-nitrosylated peptides in that backbone fragments, which retain the modification are observed.

The first two points can be explained by the modified UW mechanism proposed above (i.e., electron capture is followed by transfer to the S–N σ* orbital in direct competition with transfer to an N-Cα π* orbital). The results for $NAC_{NO}GAP-GEKWAGNDK$, $NYGLPGC_{NO}EKWYGNDK$, and $NYGLP-GEKWYGC_{NO}NDK$ suggest that initial electron capture results in $^{\bullet}NO$ loss, forming $[M - {}^{\bullet}NO + 3H]^{2+}$, followed by secondary electron capture/transfer to the N–C_α π* leading to 'typical' peptide backbone fragments, thus producing singly-charged fragments, all of which exhibit NO loss, and no doubly-charged backbone fragments.

The results for triply-charged $NYC_{NO}GLPGERWLGNDR$ and $NYC_{NO}GLPGEKYLGNDK$ (Supplementary Figure 1f and g, respectively) suggest a more even competition between transfer to the S–N σ* orbital and an amide π* orbital. The molecular structures predicted from molecular dynamics for the triply-charged species are shown in Supplemental Figure 4e–i. It is important to note that the MD simulations do not appear to have resulted in a fully converged structure for all the triply charged peptides: multiple clusters are present after 500 ns in all cases and RMSD analyses between the most representative structures between the time windows were >1 Å for four of the five peptides. As such it is difficult to draw any conclusions about the variations in behavior from these structures; however, as expected, the triply-charged peptide ions have more extended structures than their doubly-charged counterparts and since through-bond electron transfer rates have been shown to be dependent on distance [32] it may not be possible for an electron to transfer to the S–N σ* orbital due to the distance from the site of capture.

Collision-Induced Dissociation of S-Nitrosylated Peptides

The collision-induced dissociation mass spectra of the nitrosylated peptides are shown in Supplemental Figure 5. For the doubly-charged precursors, as observed by Hao and Gross [5], the dominant fragmentation channel is homolysis of the S-N bond to form a long-lived radical and $^{\bullet}NO$. In some cases additional losses, corresponding to amino acid side chains are observed. These losses are discussed in more detail below. Five of the eight doubly-charged

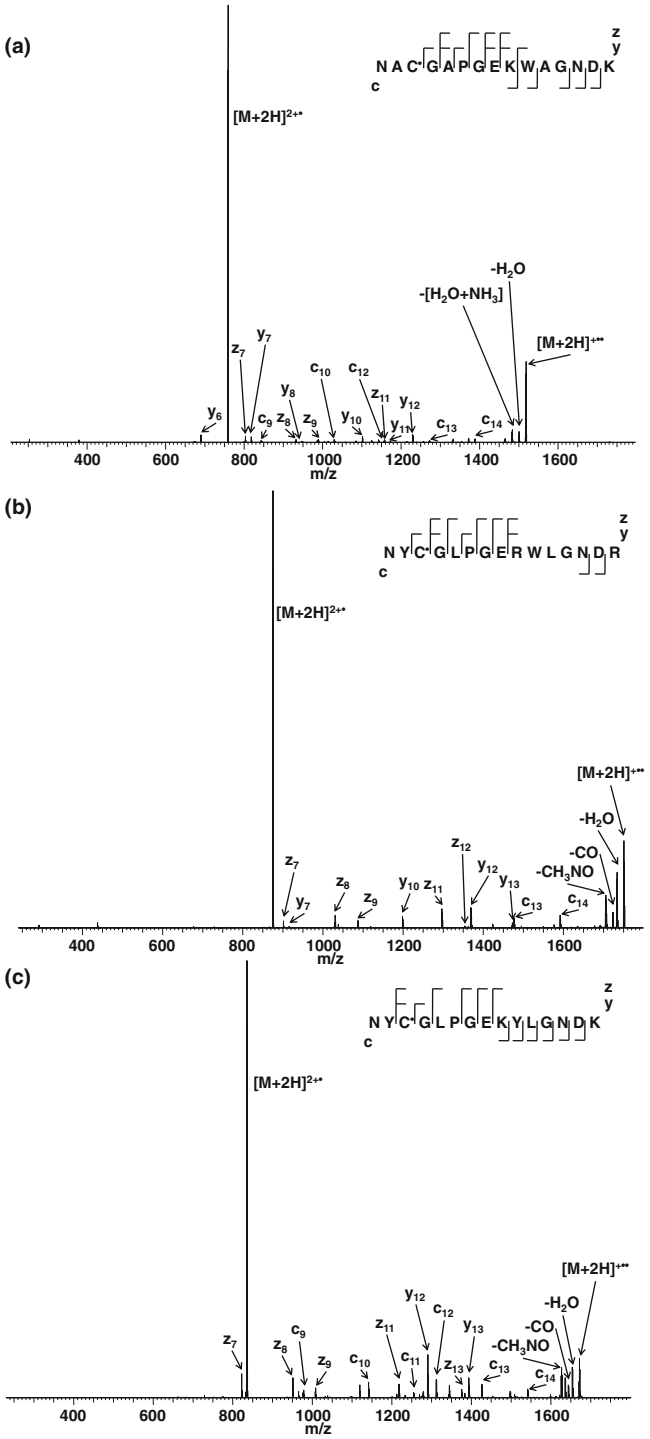

Figure 3. MS^3 (CID-ECD) mass spectra of radical peptide ions (formed following CID of the *S*-nitrosopeptide): **(a)** $[NAC^{\bullet}GAP-GEKWAGNDK + 2H]^{2+\bullet}$; **(b)** $[NYC^{\bullet}GLPGERWLGNDR + 2H]^{2+\bullet}$; **(c)** $[NYC^{\bullet}GLPGEKYLGNDK + 2H]^{2+\bullet}$ $C^{\bullet}$ denotes a sulfur atom (cysteine) radical

peptides dissociated to give the y_{10} ion (i.e. cleavage N-terminal to the proline residue [33]). CID of [NYC$_{NO}$GLP GERWLGNDR + 2H]$^{2+}$ also resulted in y_7 and b_{14} fragments, both of which derive from cleavage at the arginine residues and can be explained by the basicity of arginine in relation to the mobile proton model [33–35].

CID of the triply-charged precursors gave more extensive fragmentation. All of the peptides which contained tryptophan fragmented at that residue to give *c* and *y* ions. The *c* ions were particularly intense, with the exception of the peptide that contained two arginine residues. Four of the five peptides fragmented to give abundant [z_{14}-$^{\bullet}$NO]$^{2+}$ ions (i.e., cleavage adjacent to the N-terminal asparagine residue). Backbone fragmentation is discussed in more detail below.

MS3: CID-ECD of S-nitrosylated peptides

The ECD mass spectra of the stable radical peptide ion following $^{\bullet}$NO loss generated by CID can be seen in Figure 3 and Supplemental Figure 6. The nature of the cysteine radical has been the subject of a number of studies. On formation, the radical resides on the sulfur atom (the distonic structure). Both Zhao et al. [36] and Ryzhov et al. [22], calculated that the most stable structure was the result of hydrogen atom transfer from the α-carbon giving an α-radical stabilized by the captodative effect [37]. Nevertheless, gas-phase IR spectroscopy by Fornarini and co-workers revealed the long-lived distonic structure of the radical [28]. More recent work by Ryzhov and co-workers [27] suggests that radical migration to the α-carbon does occur. A comparison of the reactivity of the N-acetyl cysteine radical generated by in-source CID with that generated by ion trap-CID, together with IR spectroscopy of the species generated in source, suggested that within the timescale of the experiments ~30 % conversion to the α-radical occurs. More recent work has focused on larger species; Zhao et al. [38] studied the tripeptide glutathione [Glu-Cys-Gly] radical ion and found that the sulfur radical readily converts to the N-terminal α-carbon radical. Osburn et al. [39] showed that radical transfer from the sulfur atom to the α-carbon is sequence specific. Whereas limited transfer was observed for the dipeptide radical ion Cys-Gly, radical transfer was facile for Gly-Cys.

In our experiments, the radical ion was generated by ion trap CID and so we hypothesise that, at least initially, the distonic structure will dominate. ECD of [NYC$^{\bullet}$GLPGEYWLGNDK + 2H]$^{2+\bullet}$ results in a single *y* fragment, y_{12}, and [NYC$^{\bullet}$GLP-GEYWLGNDR + 2H]$^{2+\bullet}$ results in no backbone fragmentation, see Supplementary Figure 3a and b, whereas ECD of their unmodified counterparts (Supplementary Figure 2a and b) resulted in 92.9 % and 57.1 % coverage, respectively. If the radical underwent transfer to the α-carbon, as discussed above, we might expect some radical migration throughout the peptide backbone leading to *c*/*z* ion formation [40]. Nevertheless it should be noted that if radical transfer were sufficiently slow, the ions may have cooled and would not necessarily dissociate. As no fragmentation was observed, we conclude that either the radical site remains on the sulfur atom, or migrates without dissociation, and postulate that following initial capture at the N-terminus, the electron undergoes through-bond or through-space transfer to the partially occupied orbital at the radical site, precluding any further radical directed fragmentation.

The ECD mass spectra of [NAC$^{\bullet}$GAPGEKWAGNDK + 2H]$^{2+\bullet}$, [NYC$^{\bullet}$GLPGERWLGNDR + 2H]$^{2+\bullet}$, and [NYC$^{\bullet}$GLP-GEKYLGNDK + 2H]$^{2+\bullet}$ (Figure 3) reveal considerable

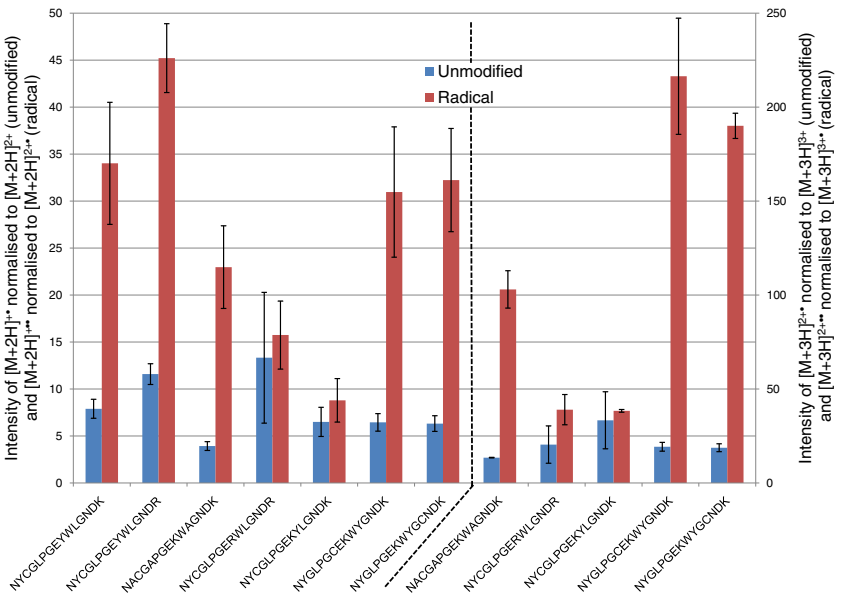

Figure 4. Comparison of the relative intensities of the ECnoD peaks following electron capture by the unmodified and radical peptide: (left) doubly-charged ions; (right) triply-charged ions. Radical peptides were formed following CID of the *S*-nitrosopeptide. Error bars constitute standard deviation of n=3

peptide sequence coverages (78.6 %, 64.3 %, and 85.7 %, respectively), which are comparable to those obtained from their unmodified counterparts (85.7 %, 92.9 %, and 85.7 %, respectively) (Supplementary Figure 2c, d, and e**)**. There are two possible explanations for their ECD behaviour. First, radical migration to the α-carbon precedes migration along the peptide backbone and backbone fragmentation (i.e., it is possible that the differences in the sequences of these peptides enable radical transfer, as seen by Osburn et al. [39]). Alternatively, there is competition between transfer of the captured electron from one of the basic residues to the radical site and to a Coulomb-stabilized amide π* orbital. In [NYGLPGC$^{\bullet}$EKWYGNDK + 2H]$^{2+\bullet}$ and [NYGLPGEK WYGC$^{\bullet}$NDK + 2H]$^{2+\bullet}$ the site of the initial sulfur radical is in close proximity to the presumed protonation sites (the basic residues). In both cases, ECD results in no fragmentation (Supplemental Figure 6c and d) in the vicinity of the radical. Similar results were obtained for the triply-charged peptides (Supplemental Figure 6e–i). ECD of [NAC$^{\bullet}$GAPGEK-WAGNDK + 3H]$^{3+\bullet}$, [NYC$^{\bullet}$GLPGERWLGNDR + 3H]$^{3+\bullet}$, and [NYC$^{\bullet}$GLPGEKYLGNDK + 3H]$^{3+\bullet}$ results in significant peptide backbone fragmentation (64.3 %, 71.4 %, and 71.4 % coverage, respectively), whereas ECD of [NYGLPGC$^{\bullet}$EK-WYGNDK + 3H]$^{3+\bullet}$, and [NYGLPGEKWYGC$^{\bullet}$NDK + 3H]$^{3+\bullet}$ gives low sequence coverage.

Perhaps the most striking feature of the MS^3 ECD mass spectra is the relative abundance of the charge-reduced species. Figure 4 shows the relative intensities of the ECnoD peaks, i.e., ratio of charge-reduced precursor ([M + 2H]$^{+\bullet\bullet}$ or [M + 3H]$^{2+\bullet\bullet}$) to the precursor ion ([M + 2H]$^{2+\bullet}$ or [M + 3H]$^{3+\bullet}$, respectively), following electron capture by the radical peptides and their unmodified counterparts. In all cases, the relative intensity of the ECnoD peak is greater for the radical peptide than its unmodified counterpart. This increase does not appear to be significant for peptides NYC$^{\bullet}$GLPGERWLGNDR and NYC$^{\bullet}$GLPGEKYLGNDK, both of which gave considerable backbone fragmentation. These results further support the proposal that following electron capture, competition exists between transfer to the sulfur radical and a Coulomb-stabilized amide π* orbital.

MS3: CID-CID of S-nitrosylated peptides

CID mass spectra of the radical peptide ions obtained following initial CID of the *S*-nitrosopeptide are shown in Figure 5 and Supplemental Figure 7. A number of fragmentation channels are observed including losses of amino acid side chains and backbone cleavage. CID of the doubly-charged radical peptide ions (Figure 5 and Supplemental Figure 7a–d) resulted in losses of $^{\bullet}$SH, C_4H_8, and $^{\bullet}CH_2NO$. Loss of NH_3 was also observed following CID of the arginine-containing peptide.

Losses of C_4H_8 have previously been observed in electron capture dissociation mass spectra and assigned to loss of a leucine or isoleucine side chain [41, 42]. (Note that C_4H_8 loss was not observed following CID of [NAC$^{\bullet}$GAP-GEKWAGNDK + 2H]$^{2+\bullet}$). The mechanism for this loss, suggested by Julian and co-workers [43], is abstraction of the γ-hydrogen from the leucine side chain followed by homolysis of the C_α–C_β. As discussed above, the initial

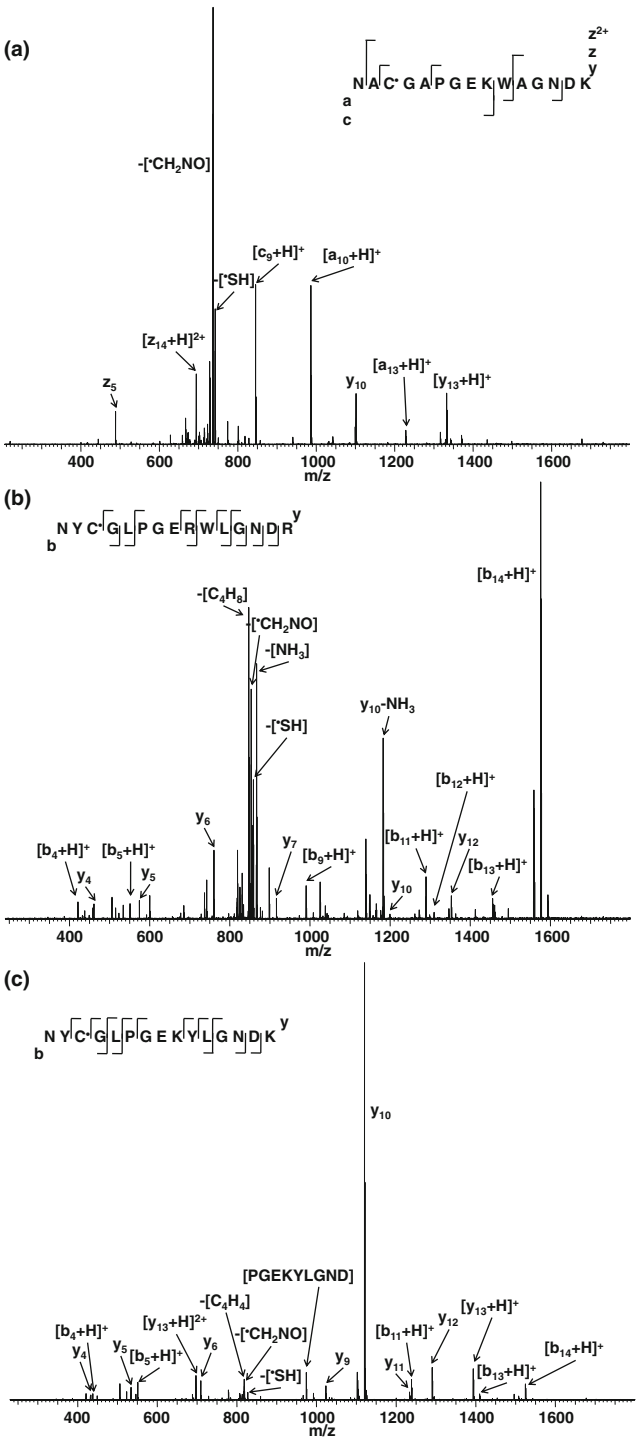

Figure 5. MS^3 (CID-CID) mass spectra of radical peptide ions (formed following CID of the *S*-nitrosopeptide): **(a)** [NAC$^{\bullet}$GAPGEKWAGNDK + 2H]$^{2+\bullet}$; **(b)** [NYC$^{\bullet}$GLP-GERWLGNDR + 2H]$^{2+\bullet}$; **(c)** [NYC$^{\bullet}$GLPGEKYLGNDK + 2H]$^{2+\bullet}$

structure of the radical peptide likely comprises the sulfur radical; however, migration to the α-carbon may occur following collisional activation. Either of these radicals may be responsible for the γ-hydrogen abstraction, which precedes C_4H_8 loss.

Losses of $^{\bullet}CH_2NO$ (specifically $^{\bullet}C(O)NH_2$) from the side chain of asparagine have also previously been observed in ECD mass spectrometry [42]. The proposed mechanism involves abstraction of the α-hydrogen and homolysis of the C_β–C_γ bond [44]. Asparagine has the lowest Cα–H bond dissociation enthalpy (BDE) of all the essential amino acids [45], thus explaining the apparent favored migration of the radical from the sulfur to the asparagine α-carbon. Loss of $^{\bullet}CH_2NO$ was not observed following CID of either $[NYC^{\bullet}GLPGEYWLGNDK + 2H]^{2+\bullet}$ and $[NYC^{\bullet}GLPGEYWLGNDR + 2H]^{2+\bullet}$, which may suggest that radical migration to one or either asparagine is affected by the location of the protons within the peptides.

Losses of $^{\bullet}SH$ were observed following CID of all of the doubly-charged radical peptide ions studied here. These losses were also observed in the MS^3 experiments of Hao and Gross [5], but were not observed following fragmentation of cysteine radical cations [22]. In the latter case, losses of H_2S were observed. Loss of $^{\bullet}SH$ can be explained by a similar mechanism to that for loss of the Asn side chain. The initial step involves migration of the radical from the sulfur to the cysteine α-carbon. Subsequent homolysis of the C_β–S bond results in a dehydroalanine residue and $^{\bullet}SH$, see Scheme 3.

CID of the radical peptide ions lead to radical-driven peptide backbone fragmentation and the formation of *a*, *c*, and *z* fragment ions. Hao and Gross [5] observed radical-driven cleavage adjacent to Ser and Thr residues. The peptides studied here do not contain those residues and radical-driven cleavage (*a* and *c* fragments) is observed adjacent to tryptophan and tyrosine residues. The mechanism proposed is abstraction of a β-hydrogen followed by cleavage of either the N–Cα bond (to give the *c* fragment) or the Cα–C_O bond (to give the *a* fragment). Complementary *z* fragments (z_5) were observed for $[NAC^{\bullet}GAPGEKWAGNDK + 2H]^{2+\bullet}$, $[NAC^{\bullet}GAPGEKWAGNDK + 3H]^{3+\bullet}$, and $[NYGLPGC^{\bullet}EKWYGNDK + 2H]^{2+\bullet}$. Favorable fragmentation of the N–Cα bond of tryptophan and tyrosine residues in radical peptide ions generated following CID of copper (II) ternary complexes has also been observed by Siu and co-workers [46]. The β C–H bond dissociation enthalpy for tryptophan is the lowest (by >20 kJ/mol) of all the essential amino acid residues [44]. Tyrosine has the fourth lowest BDE, and the second lowest of the amino acids contained in the peptides studied here. The only peptides that did not exhibit radical-driven backbone fragmentation were $[NYC^{\bullet}GLPGEKYLGNDK]$ (in both 2+ and 3+ charge states) and [NYCGLPGERWLGNDR] (in the 2+ charge state).

With the exception of $[NYC^{\bullet}GLPGEKYLGNDK]$ and doubly-charged $[NYC^{\bullet}GLPGERWLGNDR]$, all the peptides fragmented to give the z_{14}^{2+} fragment. In most cases, this fragment results from cleavage adjacent to a tyrosine residue and could be explained by β-hydrogen abstraction from the tyrosine residue as discussed above; however, the fragment was also observed in high abundance for peptide $[NAC^{\bullet}GAPGEKWAGNDK]$, suggesting that the asparagine residue and/or adjacent N-terminus directs the cleavage. The β C–H BDE of asparagine is unremarkable, lying at the approximate midpoint of the range of amino acid β BDEs [44]. However, as mentioned above, asparagine does have the lowest α C–H BDE. It is possible that the asparagine α radical fragments either via loss of the side chain (see above) or via cleavage of the peptide backbone. It is also worth noting that the most stable structures for the glutathione radical [38] and the Gly-Cys radical [39] were the N-terminal α-carbon radicals.

Surprisingly, no radical-driven backbone fragmentation was observed following CID of $[NYC^{\bullet}GLPGERWLGNDR + 2H]^{2+\bullet}$ ions. Previous work by Laskin and co-workers [47] on singly-charged arginine-containing radical cations revealed that radical-induced dissociation was promoted over charge-directed dissociation [33–35] due to sequestration of the proton on the arginine residue. Indeed, that can be observed here in a comparison of $[NYC^{\bullet}GLPGEYWLGNDK + 2H]^{2+\bullet}$ and $[NYC^{\bullet}GLPGEYWLGNDR + 2H]^{2+\bullet}$ (Supplementary Figure 7a and b): the CID mass spectrum of the Arg-containing peptide is dominated by side chain losses and *c*/*z* fragments, whereas that of the Lys-containing peptide is dominated by the y_{10} fragment. Theoretical calculations of GRW radical cations by Chu and co-workers revealed that the presence of arginine facilitated radical migration [48]. The CID spectra of $[G^{\bullet}RW]^+$ and $[GRW]^{\bullet+}$ were very similar and both contained *a* and *c* fragments. The energy barriers for isomerization of the radicals were comparable to those for their dissociation. It is possible, therefore, that in the $[NYC^{\bullet}GLPGERWLGNDR + 2H]^{2+\bullet}$ ions, in which arginine is adjacent to tryptophan, the radical is stabilized *via* isomerization.

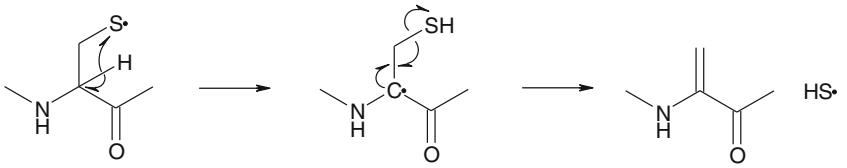

Scheme 3. Proposed mechanism of $^{\bullet}SH$ loss following CID of hydrogen-deficient radical peptide ions.

Conclusion

We have investigated the radical ion chemistry of a suite of *S*-nitrosylated peptides. ECD of doubly-charged *S*-nitrosylated peptides resulted in a striking reduction in backbone cleavage when compared with their unmodified counterparts. Greater sequence coverage was obtained for triply-charged *S*-nitrosylated peptides. Nevertheless, our results suggest that ECD is not a suitable technique for localization of *S*-nitrosylation in doubly- and triply-charged peptides. The ECD mass spectra were dominated by a peak corresponding to the loss of $^{\bullet}$NO from the charge-reduced precursor. That loss can be explained by a modified UW mechanism. Molecular dynamics simulations provided insight into the competition between electron transfer to the S–N σ^* orbital and an amide π^* orbital in these peptides. It appears that the surface accessibility of the protonation site influences the fragmentation behaviour i.e., the greater the interaction between the proton and the peptide backbone, the greater the Coulombic stabilization of the amide π^* orbital, resulting in higher backbone sequence coverage.

The dominant fragmentation pathway in the CID of the *S*-nitrosylated peptides was homolysis of the S–N bond to form a long-lived radical with loss of $^{\bullet}$NO. The radical peptide ions were isolated and subjected to ECD and CID. For ECD, the dominant pathway was electron capture with no subsequent dissociation (i.e., ECnoD). Some backbone cleavage was observed for some species. The results suggest a competition between transfer of the captured electron to the partially-filled sulfur orbital and to an amide π^* orbital. CID of the radical peptide ions resulted in losses of amino acid side chains and both radical-induced and charge-directed backbone fragmentation.

Acknowledgments

The authors (A.W.J. and H.J.C.) acknowledge EPSRC for funding. The Thermo Fisher Scientific LTQ FT Ultra mass spectrometer used in this research was obtained through the Birmingham Science City Translational Medicine: Experimental Medicine Network of Excellence project, with support from Advantage West Midlands (AWM).

References

1. Hess, D.T., Matsumoto, A., Kim, S.O., Marshall, H.E., Stamler, J.S.: Protein *S*-nitrosylation: Purview and parameters. *Nat. Rev. Mol. Cell Biol.* **6**(2), 150–166 (2005)
2. Lu, J.M., Wittbrodt, J.M., Wang, K., Wen, Z., Schlegel, H.B., Wang, P.G., Cheng, J.P.: NO affinities of *S*-nitrosothiols: A direct experimental and computational investigation of RS–NO bond dissociation energies. *J. Am. Chem. Soc.* **123**(12), 2903–2904 (2001)
3. McMillen, D.F., Golden, D.M.: Hydrocarbon Bond-Dissociation Energies. *Annu. Rev. Phys. Chem.* **33**, 493–532 (1982)
4. Singh, R.J., Hogg, N., Joseph, J., Kalyanaraman, B.: Mechanism of nitric oxide release from *S*-nitrosothiols. *J. Biol. Chem.* **271**, 18596–18603 (1996)
5. Hao, G., Gross, S.S.: Electrospray tandem mass spectrometry analysis of *S*- and *N*-nitrosopeptides: facile loss of NO and radical-induced fragmentation. *J. Am. Soc. Mass Spectrom.* **17**(12), 1725–1730 (2006)
6. Torta, F., Usuelli, V., Malgaroli, A., Bachi, A.: Proteomic analysis of protein *S*-nitrosylation. *Proteomics* **8**(21), 4484–4494 (2008)
7. Wang, Y., Liu, T., Wu, C., Li, H.: A strategy for direct identification of protein *S*-nitrosylation sites by quadrupole time-of-flight mass spectrometry. *J. Am. Soc. Mass Spectrom.* **19**(9), 1353–1360 (2008)
8. Jaffrey, S.R., Erdjument-Bromage, H., Ferris, C.D.: Tempst, Snyder, S.H. Protein *S*-nitrosylation: a physiological signal for neuronal nitric oxide. *Nat. Cell Biol.* **3**(2), 193–197 (2001)
9. Hao, G., Derakhshan, B., Shi, L., Campagne, F., Gross, S.S.: SNOSID, a proteomic method for identification of cystein *S*-nitrosylation sites in complex protein mixtures. *Proc. Natl. Acad. Sci. U.S.A.* **103**, 1012–1017 (2006)
10. Liu, M., Hou, J., Huang, L., Huang, X., Heibeck, T.H., Zhao, R., Pasa-Tolic, L., Smith, R.D., Li, Y., Fu, K., Zhang, Z., Hinrichs, S.H., Ding, S.-J.: Site-specific proteomics approach for study protein *S*-nitrosylation. *Anal. Chem.* **82**(17), 7160–7168 (2010)
11. Cooper, H.J., Hakansson, K., Marshall, A.G.: The role of electron capture dissociation in biomolecular analysis. *Mass Spectrom. Rev.* **24** (2), 201–222 (2005)
12. Zubarev, R.A., Kelleher, N.L., McLafferty, F.W.: Electron capture dissociation of multiply charged protein cations. A nonergodic process. *J. Am. Chem. Soc.* **120**(13), 3265–3266 (1998)
13. Syka, J.E.P., Coon, J.J., Schroeder, M.J., Shabanowitz, J., Hunt, D.F.: Peptide and protein sequence analysis by electron transfer dissociation mass spectrometry. *Proc. Natl. Acad. Sci. U.S.A.* **101**(26), 9528–9533 (2004)
14. Shi, S.D.H., Hemling, M.E., Carr, S.A., Horn, D.M., Lindh, I., McLafferty, F.W.: Phosphopeptide/phosphoprotein mapping by electron capture dissociation mass spectrometry. *Anal. Chem.* **73**(1), 19–22 (2001)
15. Stensballe, A., Jensen, O.N., Olsen, J.V., Haselmann, K.F., Zubarev, R.A.: Electron capture dissociation of singly and multiply phosphorylated peptides. *Rapid Commun. Mass Spectrom.* **14**(19), 1793–1800 (2000)
16. Hakansson, K., Cooper, H.J., Emmett, M.R., Costello, C.E., Marshall, A.G., Nilsson, C.L.: ECD and IRMPD MS/MS of an N-glycosylated tryptic peptide to yield complementary sequence information. *Anal. Chem.* **73**(18), 4530–4536 (2001)
17. Mirgorodskaya, E., Roepstorff, P., Zubarev, R.A.: Localization of O-glycosylation sites in peptides by ECD in a Fourier transform mass spectrometer. *Anal. Chem.* **71**(20), 4431–4436 (1999)
18. Jones, A.W., Mikhailov, V.A., Iniesta, J., Cooper, H.J.: Electron capture dissociation mass spectrometry of tyrosine nitrated peptides. *J. Am. Soc. Mass Spectrom.* **21**, 268–277 (2010)
19. Sobczyk, M., Anusiewicz, W., Berdys-Kochanska, J., Sawicka, A., Skurski, P., Simons, J.: Coulomb-assisted dissociative electron attachment: Application to a model peptide. *J. Phys. Chem. A* **109**(1), 250–258 (2005)
20. Syrstad, E.A., Turecek, F.: Toward a general mechanism of electron capture dissociation. *J. Am. Soc. Mass Spectrom.* **16**(2), 208–224 (2005)
21. Mikesh, L.M., Ueberheide, B., Chi, A., Coon, J.J., Syka, J.E.P., Shabanowitz, J., Hunt, D.F.: The utility of ETD mass spectrometry in proteomic analysis. *Biochim. Biophys. Acta–Proteins and. Proteomics* **1764**(12), 1811–1822 (2006)
22. Ryzhov, V., Lam, A.K.Y., O'Hair, R.A.J.: Gas-Phase Fragmentation of Long-Lived Cysteine Radical Cations Formed Via NO Loss from Protonated S-Nitrosocysteine. *J. Am. Soc. Mass Spectrom.* **20**(6), 985–995 (2009)
23. Lindorff-Larsen, K., Piana, S., Palmo, K., Maragakis, P., Klepeis, J.L., Dror, R.O., Shaw, D.E.: Improved side-chain torsion potentials for the Amber ff99SB protein force field. *Prot. Struct. Funct. Bioinformatics* **78**(8), 1950–1958 (2010)
24. Han, S.: An Amber Force Field for *S*-Nitrosoethanethiol That Is Transferable to *S*-Nitrosocysteine. *Bull. Korean Chem. Soc.* **31**(10), 2903–2908 (2010)
25. Feig, M., Karanicolas, J., Brooks, C.L.: MMTSB tool set: enhanced sampling and multiscale modeling methods for applications in structural biology. *J. Mol. Graphics Model.* **22**(5), 377–395 (2004)
26. Osburn, S., Steill, J.D., Oomens, J., O'Hair, R.A.J., van Stipdonk, M., Ryzhov, V.: Structure and Reactivity of the Cysteine Methyl Ester Radical Cation. *Chem. Eur. J.* **17**(3), 873–879 (2011)

27. Osburn, S., Berden, G., Oomens, J., O'Hair, R., Ryzhov, V.: Structure and Reactivity of the *N*-Acetyl-Cysteine Radical Cation and Anion: Does Radical Migration Occur? *J. Am. Soc. Mass Spectrom.* **22**(10), 1794–1803 (2011)
28. Sinha, R.K., Maitre, P., Piccirillo, S., Chiavarino, B., Crestoni, M.E., Fornarini, S.: Cysteine radical cation: a distonic structure probed by gas phase IR spectroscopy. *Phys. Chem.. Chem. Phys.* **12**(33), 9794–9800 (2010)
29. Simons, J.: Mechanisms for S–S and N–C-α bond cleavage in peptide ECD and ETD mass spectrometry. *Chem. Phys. Lett.* **484**(4/6), 81–95 (2010)
30. Li, X.H., Tang, Z.X., Zhang, X.Z.: Natural Bond Orbital Analysis of Some S-Nitrosothiols Biological Molecules. *Int. J. Quantum Chem.* **110** (8), 1565–1572 (2010)
31. Holm, A.I.S., Hvelplund, P., Kadhane, U., Larsen, M.K., Liu, B., Nielsen, S.B., Panja, S., Pedersen, J.M., Skrydstrup, T., Stochkel, K., Williams, E.R., Worm, E.S.: On the mechanism of electron-capture-induced dissociation of peptide dications from N-15-labeling and crown-ether complexation. *J. Phys. Chem. A* **111**(39), 9641–9643 (2007)
32. Sobczyk, M., Simons, J.: Distance dependence of through-bond electron transfer rates in electron-capture and electron-transfer dissociation. *Int. J. Mass Spectrom.* **253**(3), 274–280 (2006)
33. Dongre, A.R., Jones, J.L., Somogyi, A., Wysocki, V.H.: Influence of peptide composition, gas-phase basicity, and chemical modification on fragmentation efficiency: Evidence for the mobile proton model. *J. Am. Chem. Soc.* **118**(35), 8365–8374 (1996)
34. Summerfield, S.G., Whiting, A., Gaskell, S.J.: Intra-ionic interactions in electrosprayed peptide ions. *Int. J. Mass Spectrom. Ion Processes* **162** (1/3), 149–161 (1997)
35. Wysocki, V.H., Tsaprailis, G., Smith, L.L., Breci, L.A.: Special feature: Commentary—Mobile and localized protons: a framework for understanding peptide dissociation. *J. Mass Spectrom.* **35**(12), 1399–1406 (2000)
36. Zhao, J.F., Siu, K.W.M., Hopkinson, A.C.: The cysteine radical cation: structures and fragmentation pathways. *Phys. Chem.. Chem. Phys.* **10**, 281–288 (2008)
37. Viehe, H.G., Janousek, Z., Merenyi, R., Stella, L.: The Captodative Effect. *Acc. Chem. Res.* **18**(5), 148–154 (1985)
38. Zhao, J.F., Siu, K.W.M., Hopkinson, A.C.: Glutathione radical cation in the gas phase; generation, structure and fragmentation. *Org. Biomol. Chem.* **9**(21), 7384–7392 (2011)
39. Osburn, S., Berden, G., Oomens, J., O'Hair, R.A.J., Ryzhov, V.: S-to-αC Radical Migration in the Radical Cations of Gly-Cys and Cys-Gly. *J. Am. Soc. Mass Spectrom.* **23**(6), 1019–1023 (2012)
40. Leymarie, N., Costello, C.E., O'Connor, P.B.: Electron capture dissociation initiates a free radical reaction cascade. *J. Am. Chem. Soc.* **125**(29), 8949–8958 (2003)
41. Cooper, H.J., Hudgins, R.R., Hakansson, K., Marshall, A.G.: Secondary fragmentation of linear peptides in electron capture dissociation. *Int. J. Mass Spectrom.* **228**, 723–728 (2003)
42. Fung, Y.M.E., Chan, T.W.D.: Experimental and theoretical investigations of the loss of amino acid side chains in electron capture dissociation of model peptides. *J. Am. Soc. Mass Spectrom.* **16**(9), 1523–1535 (2005)
43. Moore, B.N., Ly, T., Julian, R.R.: Radical Conversion and Migration in Electron Capture Dissociation. *J. Am. Chem. Soc.* **133**(18), 6997–7006 (2011)
44. Sun, Q.Y., Nelson, H., Ly, T., Stoltz, B.M., Julian, R.R.: Side Chain Chemistry Mediates Backbone Fragmentation in Hydrogen Deficient Peptide Radicals. *J. Proteome Res.* **8**(2), 958–966 (2009)
45. Rauk, A., Yu, D., Taylor, J., Shustiv, G.V., Block, D.A., Armstrong, D.A.: Effects of structure on C-α–H bond enthalpies of amino acid residues: relevance to H transfers in enzyme mechanisms and in protein oxidation. *Biochemistry* **38**(28), 9089–9096 (1999)
46. Siu, C.K., Ke, Y.Y., Orlova, G., Hopkinson, A.C., Siu, K.W.M.: Dissociation of the N–C_α Bond and Competitive Formation of the $[z_n - H]^{\bullet+}$ and $[c_n\ 2H]^+$ Product Ions in Radical Peptide Ions Containing Tyrosine and Tryptophan: The Influence of Proton Affinities on Product Formation. *J. Am. Soc. Mass Spectrom.* **19** (12), 1799–1807 (2008)
47. Laskin, J., Yang, Z., Ng, C.M.D., Chu, I.K.: Fragmentation of alpha-radical cations of arginine-containing peptides. *J. Am. Soc. Mass Spectrom.* **21**, 511–521 (2010)
48. Song, T., Ng, D.C.M., Quan, Q.A., Siu, C.K., Chu, I.K.: Arginine-Facilitated alpha- and pi-Radical Migrations in Glycylarginyltryptophan Radical Cations. *Chem. Asian J.* **6**(3), 888–898 (2011)